Continuous Coherent Lyman-α Excitation of Atomic Hydrogen

K. S. E. Eikema,* J. Walz,† and T. W. Hänsch
Max-Planck-Institut für Quantenoptik, Hans-Kopfermann-Strasse 1, 85748 Garching, Germany
(Received 21 February 2001)

The $1S$-$2P$ transition in atomic hydrogen has been observed for the first time with almost natural linewidth. We employ a unique source of continuous coherent Lyman-α radiation based on four-wave mixing in mercury. The output of the source has been improved 40-fold to yield 20 nW. This demonstration shows that laser cooling and detection with continuous Lyman-α radiation has excellent prospects for future experiments with antihydrogen.

DOI: 10.1103/PhysRevLett.86.5679 PACS numbers: 32.30.Jc, 32.70.Jz, 32.80.Pj, 42.65.Ky

The search for physics beyond the standard model is a strong inspiration to test the *CPT* symmetry to ultrahigh precision. Properties such as inertial mass, magnetic moment, or charge/mass ratios [1] have been compared between elementary particles and their antimatter equivalent. Low energy atomic antimatter would open a new field of testing *CPT* by comparing properties of internal atomic structure [2,3]. It would possibly even make the experimental observation of the effect of gravity on antimatter feasible [4,5]. The recent trapping and cooling of both antiprotons and positrons at CERN's new antiproton-decelerator (AD) [6] and the progress in producing atoms from ions and electrons [7] indicate that creation of cold antihydrogen could be imminent. Besides magnetic confinement, optical means of measurement and manipulation of the antiatoms will play a pivotal role as any contact with matter results in rapid annihilation. The $1S$-$2P$ transition is the first and strongest transition suitable for fluorescence detection and laser cooling of magnetically confined antihydrogen in the ground state. However, producing radiation at the required wavelength of 121.56 nm (Lyman-α) in the vacuum ultraviolet (VUV) is still a challenge.

In this Letter, we report on the first near-natural linewidth atomic hydrogen excitation of the $1S$-$2P$ transition. The results obtained with hydrogen are a direct measure of what can be achieved with antihydrogen as the internal energy structure is expected to be the same to high precision. To induce the $1S$-$2P$ transition we use a significantly improved continuous coherent Lyman-α source. Laser cooling and spectroscopy with *pulsed* Lyman-α has been demonstrated for magnetically trapped hydrogen [8] before. However, the use of a *continuous* source of Lyman-α is strongly preferred as it allows for more efficient laser cooling without saturation and has a more favorable duty cycle of 100%. The bandwidth is far superior to pulsed sources, which allows for a higher selectivity of sublevels in a magnetic trap. This should enable low-loss laser cooling to the Doppler limit of 2.4 mK.

Our source of Lyman-α radiation (see Fig. 1) is based on continuous four-wave mixing (FWM) in natural mercury vapor which produces the sum frequency of three incident laser beams [9]. We employ fundamental beams at wavelengths of 257 and 399 nm for an exact two-photon resonance with the $7s\ ^1S_0$ state of mercury (mass 202 isotope, 30% abundance). The third incident beam is at a wavelength of 545 nm, to reach the photon energy of Lyman-α, and originates from a Rhodamine 110 dye laser. Both ultraviolet (UV) wavelengths are produced by frequency doubling in x-folded enhancement resonators. Up to 850 mW of light at 257 nm is generated this way in a BBO crystal from a 2.2 W single-mode argon-ion laser at 514.5 nm. A similar resonator containing LBO as nonlinear crystal is used to frequency double a single-mode frequency-stabilized Ti:sapphire laser. From 2.05 W at 798 nm, up to 920 mW of 399 nm light has been produced. Both crystals are heated to 50 °C, and flushed with dust-free oxygen to protect the surfaces from degradation. VUV radiation is generated by strongly focusing the three fundamental beams with a single fused silica lens (L1, $f = +15$ cm) in a vapor zone of mercury. All beams have the same parallel polarization.

Beam quality and overlap of all three beam waists is critical. The astigmatism of the beams produced by frequency doubling is therefore compensated by cylindrical

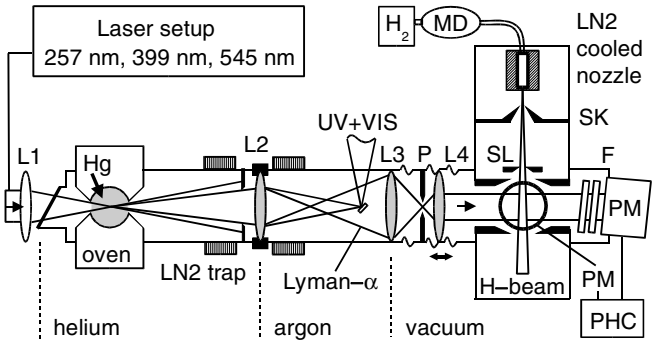

FIG. 1. Schematic of the setup for continuous Lyman-α generation and $1S$-$2P$ atomic hydrogen spectroscopy. In this figure VIS + UV stands for the fundamental laser beams, L1 for a quartz lens, while L2–L4 are MgF_2 lenses, SL for slit, F for two Lyman-α filters, PM for solar-blind photomultiplier, MD for microwave dissociator, PHC for photon counting, SK for skimmer, P for pinhole, and LN2 for liquid nitrogen.

lenses. Telescopes with spatial filtering are employed to ensure equal focusing properties of lens L1. The average Rayleigh length is ≈0.8 mm, which is 2 to 3 times larger than the diffraction limit due to the non-Gaussian intensity profiles and limitations of especially the astigmatism compensation optics.

The interaction zone with mercury vapor is only 15 mm long and is produced in a specially designed mercury oven. The mercury pressure is inferred from temperature measurements and can be set up to 40 mbar (220 °C). A buffer gas of ≈70 mbar helium in the oven ensures that the surrounding optics remain free of mercury. In our previous experiment we observed an oscillatory structure of the VUV yield curve [9]. This was ascribed to strong Lyman-α absorption due to mercury dimers. Our new mercury oven has a 3 times smaller interaction zone and in addition a near rectangular density profile. No oscillatory structure of the VUV yield curve has been observed with the new mercury oven, indicating that the influence of VUV absorption has been overcome to a large extent.

To measure the VUV yield and to perform $1S$-$2P$ spectroscopy, the intensity of the fundamental beams has to be suppressed by many orders of magnitude. For this purpose we use the chromatic aberration of a MgF_2 lens (L2). VUV light focuses after lens L2 at an almost 2 times shorter distance than the fundamental beams. In this manner most of the VUV can pass a tiny (3 mm) mirror placed in the focus of the fundamental wavelengths. Although the mirror casts a shadow (≈20% intensity loss) in the VUV beam, the colinear arrangement is very convenient for the alignment of the apparatus. Lens L2 has been one of the most critical objects in the setup. Without special measures taken, the high power 257 nm beam induces a rapid buildup of contaminants on the surface of the lens. As some parts of the setup cannot be baked, we assume that the deposits consist of organic molecules which can absorb virtually all VUV radiation. This effect strongly limited the sustainable VUV power that could be produced before [9]. We now solved this problem by using liquid nitrogen traps around the lens. Furthermore, the lens itself is mounted with indium seals and heated to 65 °C. In addition, argon buffer gas is used in the middle section to reduce diffusion of contaminant molecules. As a final measure we exploit the fact that the VUV beam has a ≈1.7 times smaller divergence than the fundamental beams. Only the central part of the beam containing the VUV is therefore led through and fills the lens of 20 mm effective diameter, so that the UV intensity is kept as low as possible. These combined steps make it now possible to operate the source for many weeks at full power without any degradation of the VUV output.

To measure the VUV yield a solar-blind photomultiplier (Hamamatsu R1459) was placed directly after the first MgF_2 lens and the tiny mirror, with 3 narrow bandwidth Lyman-α filters (Acton Research) in front of it. Corrected for the detection efficiency of 2.4×10^{-4} we achieved a maximum yield at Lyman-α of 20 nW (1.2×10^{10} photons/s) in 22 mbar Hg. This yield is nearly constant over a Hg pressure range of 20 to 40 mbar. The fundamental laser power in the interaction zone was 570 mW at 257 nm, 500 mW at 399 nm, and 1.2 W at 545 nm. The VUV yield is strongly wavelength dependent (see Fig. 3 in Ref. [9]) due to the level structure of mercury and phase matching effects. As a result up to 10 times more VUV at 122.1 nm can be produced (200 nW), which is the highest yield reported so far by several orders of magnitude compared to continuous FWM in other metal vapors at these short wavelengths.

Application of the Lyman-α beam for $1S$-$2P$ spectroscopy requires further suppression of the fundamental UV wavelengths. Therefore the Lyman-α beam is focused first through a 0.5 mm pinhole with lens L3 to reduce Lyman-α and UV stray light. This pinhole typically transmits 90% of Lyman-α, and reduces UV light by at least 2 orders of magnitude. A third MgF_2 lens (L4) collimates the Lyman-α beam after which it crosses a beam of atomic hydrogen. Blackened guiding tubes reduce stray light and leave a gap of 16 mm wide for the hydrogen beam and fluorescence detection. Because of the three lenses and the pinhole, 5% to 10% of the generated Lyman-α reaches the interaction zone (≈1−2 nW).

A beam of hydrogen is produced in a differentially pumped chamber by microwave dissociation of H_2 at 0.5 mbar. The atomic hydrogen is channeled through Teflon tubing and emanates from a 0.5 mm diameter nozzle. This nozzle is cooled with liquid nitrogen, and constructed with an inner surface of 0.5 mm thick Teflon to reduce recombination to molecular hydrogen. A skimmer of 1 mm diameter orifice and at 20 mm distance from the nozzle is used for differential pumping. Both the source and interaction chamber are pumped by two cascaded turbo pumps.

Accurate collimation of both the Lyman-α and atomic beam is required to measure the $1S$-$2P$ with a near-natural linewidth of ≈100 MHz. Hydrogen at 1 K already results in a Doppler broadening of 1 GHz. Near-natural linewidth can be accomplished only for an effective transversal temperature below a few mK. To achieve this goal the hydrogen beam is strongly collimated by a 0.3 mm narrow slit just before the interaction zone. Given the distance to the nozzle of ≈280 mm, this amounts to an effective collimation of ≈1:400. The Lyman-α beam divergence is minimized by adjusting collimation lens L4 until the recorded $1S$-$2P$ resonance line shows no further narrowing.

Figure 2 shows the excitation scheme in hydrogen. Almost all of the measurements have been performed on the (strongest) $1\ ^2S_{1/2}$-$2\ ^2P_{3/2}$ transition that can be used for laser cooling. The ground state hyperfine splitting of 1420.4 MHz can be resolved easily. The hyperfine structure of the $2P$ states is smaller than the natural linewidth. However, as indicated in Fig. 2, from $F = 0$ only the $F' = 1$, and from $F = 1$ mainly the $F' = 2$ component

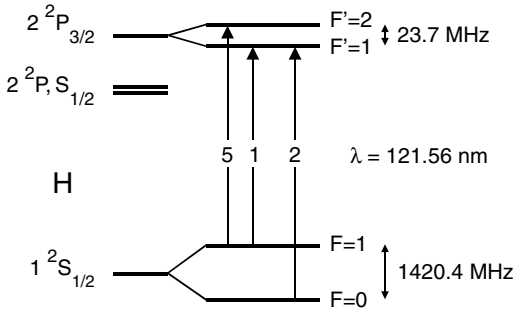

FIG. 2. Excitation scheme for $1S$-$2P$ spectroscopy in hydrogen (not drawn to scale). The numbers in the arrows indicate the relative transition intensity; the natural width of the $2P$ is 99.7 MHz.

of the $2P$ state is excited. As a result, the expected double peak separation for excitation to the $2\,^2P_{3/2}$ is 1400.5 MHz, 20 MHz smaller than the ground state hyperfine splitting.

A $1S$-$2P$ excitation spectrum is obtained by photon counting the resulting fluorescence with a solar-blind photomultiplier (Hamamatsu R1459, 23 mm diameter). It is placed 22 mm above the interaction region, perpendicular to the Lyman-α and atomic beam. Another solar-blind photomultiplier is placed directly in the Lyman-α beam to measure the generated VUV intensity. That photomultiplier has two narrow-bandwidth filters (each with Lyman-α transmission $\approx$17%, 257 nm blocking >1:200) in front to suppress spurious UV signal.

In Fig. 3 a typical experimental $1S$-$2P$ spectrum out of 24 recordings is shown. A full spectrum takes about 10 min to record. On resonance a maximum signal count rate of 1.2 kHz has been observed. Fitting the measured lines with a Lorentzian results in widths of 119(2) and 120(3) MHz for excitation from the F = 1 and F = 0 hyperfine states, respectively. A 2 MHz larger linewidth is expected for the F = 1 transition compared to the F = 0 transition, but this difference is smaller than the experimental accuracy. The expected double peak structure separation of 1400.5 MHz is reproduced to high accuracy with a measured value of 1396(6) MHz. These results clearly demonstrate the great potential for continuous Lyman-α laser cooling and spectroscopy. It should be noted that no special measures were taken yet to stabilize the Lyman-α frequency. Stability and scan range was checked by recording the markers of an etalon (free spectral range 750 MHz) in the 545 nm beam, relative to the $1S$-$2P$ resonances. Analysis of the 24 recordings showed that drifts up to 12 MHz occurred over the period between the two peaks in the $1S$-$2P$ spectrum. On average, however, correction for drift had only limited influence on the measured transition width (3 MHz) or splitting (1 MHz).

The bandwidth of the Lyman-α light hardly contributes to the measured $1S$-$2P$ linewidth, as it is expected to be well below 10 MHz. This estimation is based on the bandwidths of the fundamental beams which are each less than

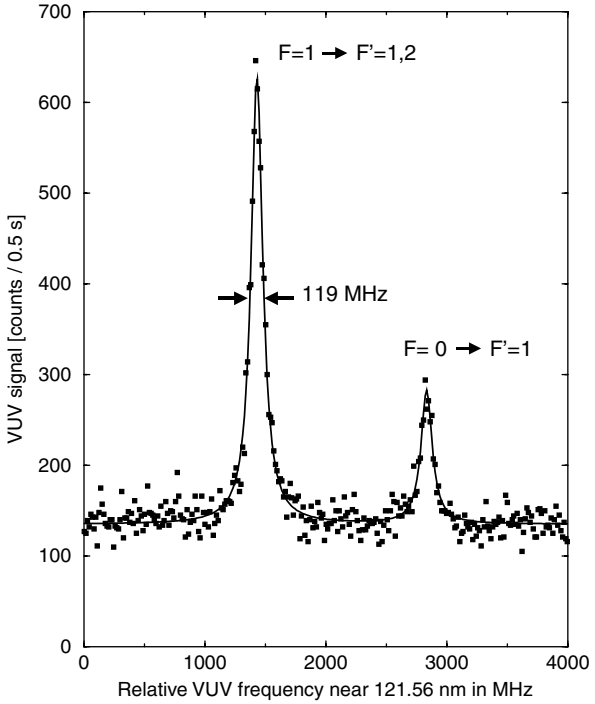

FIG. 3. Recording of the $1s\,^2S_{1/2}$-$2p\,^2P_{3/2}$ transition in a beam of atomic hydrogen with continuous coherent Lyman-α (gate time 0.5 s per data point). The solid line is a Lorentzian fit.

a few MHz. Transit-time and magnetic field ($B < 40\ \mu$T) broadening is negligible, so that the Doppler effect is mainly responsible for excess transition width. Gaussian-like broadening is therefore expected, dominated by the velocity spread of the hydrogen atoms in combination with a deviation from perfect perpendicular alignment and residual Lyman-α divergence. Convolution of a 100 MHz Lorentzian with a 55 MHz Gaussian gives a good agreement with the measured width and shape. As a rough measure, an atom-flux corrected velocity of 1400 m/s with a spread of 1250 m/s can be assumed for our liquid-nitrogen cooled hydrogen source [10]. A deviation of just 5 mrad from perpendicular alignment is then enough to account for the measured linewidth.

Initially, a strong reduction of VUV yield hampered Lyman-α spectroscopy severely. The loss of VUV intensity was seen exactly and only at the $1S$-$2P$ wavelength, even without any hydrogen beam present. Each time after an oven pump-down and filling cycle, the intensity loss increased from initially $\approx$40% to more than 99% after a few hours of operation. Several tests revealed this was due to a reaction in the laser focus of excited mercury in the $6p\,^3P$ state with spurious molecular hydrogen. This reaction results in HgH (see, e.g., Ref. [11]) and atomic hydrogen, which in turn absorbs Lyman-α radiation. The molecular hydrogen was traced back to hydrogen contamination of the stainless steel from which the oven is made. After an elaborate baking procedure at 400 °C the losses at

Lyman-α could be reduced to less than 20%, even after many hours of operation.

Our continuous source of Lyman-α has almost reached the average power of the pulsed source [8] which was previously used for laser cooling atomic hydrogen. Further improvement is still very desirable as it directly translates into faster laser cooling and more sensitive detection of antihydrogen. When natural mercury is replaced with isotopically pure mercury, 1 order of magnitude in power can be gained. The high cost has prohibited the realization of this idea so far. Another option is to increase the fundamental laser power and improve beam quality. This could be accomplished by changing to a solid-state laser system, and possibly by an enhancement cavity for 545 nm (see, e.g., [12]). The attainable improvement can be limited by ground state depletion when it is faster than the typical decay times of the excited states (10–100 ns), and diffusion of new atoms into the focal region (time scale <1 μs).

Experimentally, the saturation behavior has been investigated for the three fundamental wavelengths by varying the individual intensities over roughly 2 orders of magnitude. No clear sign of saturation was seen within the accuracy of the measurement. To compare these results with theory we calculated the Lyman-α power, based mainly on Ref. [13], for the maximum mercury pressure (40 mbar) and laser power (see above) we can attain in the current oven. A maximum of $\approx$30 nW is predicted for focusing to a Rayleigh-length of 0.6 mm. The experimental yield compares rather well with this calculation, especially given the less than ideal focusing properties of the fundamental beams at present. The highest VUV yield is expected for even tighter focusing and higher mercury density to maintain phase matching. However, this is a difficult combination to achieve, and at high density the pressure broadening of the $7s\ ^1S_0$ state will reduce the crucial two-photon resonant enhancement. Saturation due to ground state depletion can be estimated based on the maximum rates per atom in the center of a focus with 0.8 mm Rayleigh-length (assuming Gaussian beams). The calculated one-photon absorption rate is $1.1 \times 10^3\ \mathrm{s}^{-1}$ (pressure broadened at 40 mbar Hg [14]), and the two-photon absorption rate is $3.6 \times 10^3\ \mathrm{s}^{-1}$ (Doppler broadened, hyperpolarizability from [13]). Both rates are much lower than that of the relaxation processes, and do not cause significant saturation. The measured 556 nm power dependence of the VUV production peak at 122.1 nm, however, does show some indication of saturation. Further investigations are required, as it cannot be explained by either photomultiplier saturation or three-photon absorption.

In conclusion, we have measured the $1S$-$2P$ transition in hydrogen with near-natural linewidth for the first time. The continuous Lyman-α source yield has been improved forty-fold, and further headroom for at least 2 orders of magnitude more clearly exists. Given the low signals initially expected for high precision $1S$-$2S$ excitation of antihydrogen, the $1S$-$2P$ transition could serve as an alternative means for first spectroscopy of trapped antimatter in the ground state, or for sensitive detection of the $1S$-$2S$ transition in a shelving scheme [15]. This work is supported by the MPG and BMBF.

*Present address: Vrije Universiteit, Amsterdam, The Netherlands.

†Present address: CERN, Geneva, Switzerland.

[1] G. Gabrielse *et al.,* Phys. Rev. Lett. **82**, 3198 (1999); *CPT and Lorentz Symmetry,* edited by V. A. Kostelecký (World Scientific, Singapore, 1999); G. Gabrielse, Adv. At. Mol. Opt. Phys. **45**, 1 (2001).

[2] See, e.g., J. Eades and F. J. Hartmann, Rev. Mod. Phys. **71**, 373 (1999).

[3] R. Bluhm, V. A. Kostelecký, and N. Russell, Phys. Rev. Lett. **82**, 2254 (1999).

[4] J. S. Bell, in *Fundamental Symmetries,* edited by P. Bloch, P. Pavlopoulos, and R. Klapisch (Plenum, New York, 1987), p. 1.

[5] G. Gabrielse, Hyperfine Interact. **44**, 349 (1988).

[6] ATRAP Collaboration, G. Gabrielse *et al.,* Phys. Lett. B **507**, 1 (2001).

[7] C. Wesdorp, F. Robicheaux, and L. D. Noordam, Phys. Rev. Lett. **84**, 3799 (2000).

[8] I. D. Setija *et al.,* Phys. Rev. Lett. **70**, 2257 (1993).

[9] K. S. E. Eikema, J. Walz, and T. W. Hänsch, Phys. Rev. Lett. **83**, 3828 (1999).

[10] A. Huber *et al.,* Phys. Rev. A **59**, 1844 (1999).

[11] C. Jouvet and B. Soep, Laser Chem. **5**, 157 (1985).

[12] J. Nolting and R. Wallenstein, Opt. Commun. **79**, 437 (1990).

[13] A. V. Smith and W. J. Alford, J. Opt. Soc. Am. **4**, 1765 (1987).

[14] R. E. Drullinger, M. M. Hessel, and E. W. Smith, J. Chem. Phys. **66**, 5656 (1977).

[15] T. W. Hänsch and C. Zimmermann, Hyperfine Interact. **76**, 47 (1993).